Energy Conversion and Management xxx (2017) xxx–xxx

Contents lists available at ScienceDirect

Energy Conversion and Management

journal homepage: www.elsevier.com/locate/enconman

Novel method for determining optimal heat-exchanger layout for heat recovery steam generators

Mislav Čehil, Stjepko Katulić *, Daniel Rolph Schneider

Faculty of Mechanical Engineering and Naval Architecture, University of Zagreb, Ivana Lučića 5, 10000 Zagreb, Croatia

ARTICLE INFO

Article history:
Available online xxxx

Keywords:
Combined-cycle power plant
Bottom cycle
Heat recovery steam generator
Pinch point
Heat-exchanger layout

ABSTRACT

A new method for determining the optimal heat-exchanger layout in a heat recovery steam generator and its operating parameters are presented in this paper. A robust mathematical model is developed, where arbitrary steam-pressure levels and steam-reheating levels can be set. The method considers all the possible heat-exchanger layouts, in both serial and parallel arrangements of steam pressure levels or steam reheating levels. The maximum thermodynamic efficiency of the steam-turbine cycle is set as the objective function. The results show that the optimal high pressure in heat recovery steam generator without reheating is in the region of subcritical pressures, whereas that for a heat recovery steam generator with reheating is in the region of supercritical pressures. In the case of similar water or steam temperature profiles in the heat exchangers of different steam pressure levels or reheating level, from a thermodynamic viewpoint, it is justified to use a parallel heat-exchanger arrangement.

© 2017 Elsevier Ltd. All rights reserved.

1. Introduction

The electrical energy consumption in the world increases each year, i.e., the consumption of fossil fuels increases yearly. The use of fossil fuels causes greenhouse gas emissions such as CO_2 emissions, which, according to many scientists, are one of the main causes of climate change. To reduce CO_2 emissions, the European Union (EU) imposed the "2020 Climate & Energy Package," which is a set of binding legislations for ensuring that the EU meets its climate and energy targets by the year 2020. The main goals of this legislation are a 20% reduction in greenhouse-gas emissions, a 20% improvement in energy efficiency, and obtaining 20% of total produced energy from renewables [1]. The need to improve the thermodynamic efficiency of the combined-cycle power plant (CCPP) is emerging as one of the measures of the proposed EU 2020 package for increasing energy efficiency.

The best modern CCPPs achieve a thermodynamic efficiency of above 60%. Examples are CCPP Irsching 4 in Germany with a thermodynamic efficiency of 60.4% [2] and CCPP Bouchain in France with a thermodynamic efficiency of 62.22% [3]. The thermodynamic efficiency of the CCPP (η_{CCPP}) can be increased in two ways: by increasing the thermodynamic efficiency of the gas-turbine part of the power plant (η_{GT}) or by increasing the thermodynamic efficiency of the steam-turbine part of the power plant (η_{ST}). However, not every increase in η_{GT} or η_{ST} results in a corresponding increase of η_{CCPP}, because increasing η_{GT} does not necessarily increase η_{ST} . The same is valid for an increase in η_{ST}. There is an optimal change in η_{GT}/η_{ST} that results in an increase in η_{CCPP} [4]. Contemporary CCPPs have an almost continuous expansion curve in the gas-turbine part of the cycle, that ranges from approximately 1500 to 600 °C and continue in the steam-turbine part of the cycle, from 600 to 25 °C. Minimal disruption exists, only because of the necessary temperature difference between the flue gas and the fresh steam at the steam-generator outlet. In a heat recovery steam generator (HRSG), unlike in a conventional steam generator, the temperature difference between the inlet flue gas and the fresh steam is relatively small; thus, it comes to pinch-point occurrence [5]. The diagram in Fig. 1 shows the relationship between the temperature profile of the flue gas and working fluid and the exchanged heat flux. In this case, the working fluid enters an HRSG with a temperature of 25 °C, and the flue gas enters the HRSG with a temperature of 600 °C. The flue-gas temperature decreases as it transfers heat to the working fluid, whose temperature increases. At the saturation temperature, the temperature profile of the working fluid (subcritical pressures) remains constant, i.e., the working fluid evaporates. During the evaporation, the specific heat capacity of the working fluid becomes infinite. Because of this phenomenon, which affects the working-fluid temperature profile, it can be said that the pinch point is the result of the increase in the specific heat capacity of water heated in the economizer and

* Corresponding author.
E-mail addresses: mcehil@fsb.hr (M. Čehil), skatulic@fsb.hr (S. Katulić), daniel.schneider@fsb.hr (D.R. Schneider).

http://dx.doi.org/10.1016/j.enconman.2017.03.033
0196-8904/© 2017 Elsevier Ltd. All rights reserved.

Please cite this article in press as: Čehil M et al. Novel method for determining optimal heat-exchanger layout for heat recovery steam generators. Energy Convers Manage (2017), http://dx.doi.org/10.1016/j.enconman.2017.03.033

Nomenclature

g_{rad}	HRSG radiation heat losses to the environment
DP	double pressure
fg	flue gas
FP	feed pump
h	enthalpy [J/kg]
HP	high pressure
i,k	pressure-level index
IP	intermediate pressure
j	reference to the HRSG element within individual pressure level
LP	low pressure
P_{FP}	feed-pump electrical power [W]
P_{ST}	steam-turbine electrical power [W]
q_m	mass flow, [kg/s]
RH	reheating
SH	superheating
SP	single pressure
TP	triple pressure
wf	working fluid
x_i	proportion of mass flow of lower pressure levels compared to mass flow of HP pressure level
Δh	enthalpy increment [J/kg]
ΔT_{PP}	pinch point
η_{CCPP}	thermodynamic efficiency of CCPP
η_{GT}	thermodynamic efficiency of gas-turbine part of power plant
η_{HRSG}	thermodynamic efficiency of HRSG
η_{SC}	thermodynamic efficiency of steam-turbine cycle
η_{ST}	thermodynamic efficiency of steam-turbine part of power plant
Φ_{GT}	outlet gas turbine heat flux [W]
$\Phi_{HRSG,ex}$	heat flux exchanged in HRSG [W]
$\Phi_{HRSG,in}$	inlet heat flux to the HRSG [W]

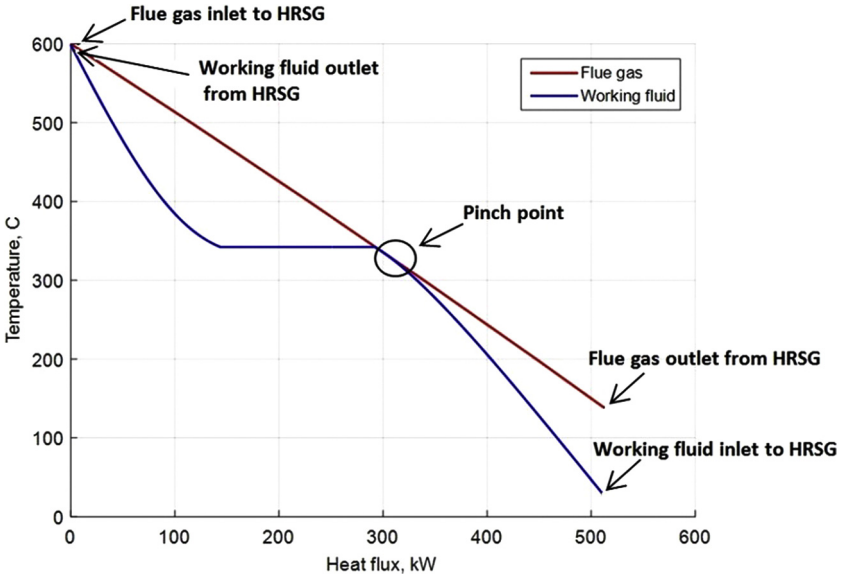

Fig. 1. Flue gas and working fluid temperature profiles inside an HRSG.

its infinite value during evaporation on one hand and a result of the small temperature difference between the inlet flue gas and the fresh steam on the other hand. The increase of the aforementioned temperature difference always reduces the pinch-point effect. A consequence of the pinch-point effect is the inability to cool the flue gas to temperatures close to the inlet feed water temperature.

This reduces the thermodynamic efficiency of the HRSG (η_{HRSG}). Thus, to achieve a high η_{ST}, it is necessary for the η_{HRSG} and the thermodynamic efficiency of the steam cycle (η_{SC}) to be high, which are mutually opposing parameters in HRSGs. Therefore, it is necessary to determine the optimal relationship between these two values. This optimal relationship between η_{HRSG} and η_{SC} can be achieved only via the simultaneous optimization of the heat-exchanger layout of the HRSG and the working-fluid parameters (pressure, temperature, mass flow). Modern HRSGs have more than one pressure level. Additional pressure levels offer lower pressures and lower superheating temperatures. They allow further utilization of the flue-gas waste heat in contrast to systems with only one pressure level [6]. Unfortunately, the η_{SC} of these additional pressure levels is lower than the η_{SC} of the first pressure level. Many studies have been performed on the optimization of a CCPP. Some studies use a thermoeconomic approach, which is a compromise between improving the thermodynamic efficiency and reducing investment costs. Valdes et al. [7] optimized the combined cycle with HRSGs having one and more pressure levels, using the production cost per unit of generated electricity and the annual cash flow as objective functions. Optimizing the heat-exchanger layout was not an aim of their work. They optimized only the working parameters, such as the pressure and temperature. Katovicz and Bartela [8] optimized a HRSG with triple-pressure (TP) steam and a reheater, analyzing the influence of the fuel price on the optimum operating parameters. The objective function was the net present value of investment. They did not optimize the heat-exchanger layout. Rahim [9] performed a sensitivity analysis for single, double, and TP HRSGs in a CCPP. They performed a parametric analysis of the influence of the working parameters on the

Please cite this article in press as: Čehil M et al. Novel method for determining optimal heat-exchanger layout for heat recovery steam generators. Energy Convers Manage (2017), http://dx.doi.org/10.1016/j.enconman.2017.03.033

thermodynamic efficiency of a CCPP. Feng et al. [10] optimized three different layouts of a dual-pressure HRSG. Naemi et al. [11] optimized the performance of an HRSG using different objective functions (exergy waste and exergy destruction). They only optimized the working parameters. Tajik Mansouri et al. [12] studied different configurations of HRSGs with two and three pressure levels and the same gas turbine as the topping cycle (Brayton cycle) and evaluated the exergy efficiency of each configuration. Rovira et. al. [13] developed a thermoeconomic optimization model whose objective function minimized the price of electricity, considering that power plants often operate with a partial load. More complex optimization methods based on exergoenergetic analyses are also the focus of researchers. Exergoeconomic theory combines the second law of thermodynamics [14] with economic principles in order to consider the cost of thermodynamic imperfections (losses) in the total cost of running a power plant [15]. In recent years, interest in the exergoeconomic optimization of power-plant operation has grown, including cogeneration systems [16] and systems with renewable energy sources [17]. Ahmadi and Dincer [18] applied exergoeconomic theory for the optimization of a CCPP with two pressure levels of steam and additional fuel combustion while observing the impact of fuel prices on the optimization parameters. Petrakopoulou et al. [19] performed a thorough exergoeconomic analysis to determine the potential benefits of using a system with TP steam. Carapelluci and Giordano [20] applied two methods for optimizing the operating parameters of a CCPP: a) minimizing the cost per unit of generated electricity and b) minimizing the objective function representing exergoeconomic losses associated with thermodynamic irreversibility. The optimization was performed for different configurations of combined power plants with different pressure levels of steam, different gas turbines, and different fuel prices.

Thus far, no studies have involved the simultaneous optimization of the HRSG heat-exchanger layout and the operating parameters of each pressure level. The proposed simultaneous optimization is essential for determining the HRSG configuration of a CCPP topping cycle, which allows the determination of the optimal thermodynamic efficiency of a power plant. The mathematical model described in this paper allows the determination of the optimal HRSG heat-exchanger layout (heat exchangers of each pressure level can be in their mutual parallel and/or serial positions) and working parameters by using a genetic algorithm as the main optimization algorithm.

2. Mathematical model

The relationship between the thermodynamic efficiencies of the steam-turbine cycle, gas-turbine cycle, and combined power plant is given by the following equation:

$$\eta_{CCPP} = \eta_{GT} + (1 - \eta_{GT}) \cdot \eta_{ST} \quad (1)$$

From a mathematical viewpoint, Eq. (1) is a function of two equally significant variables and can be rewritten as

$$\eta_{CCPP} = \eta_{ST} + (1 - \eta_{ST}) \cdot \eta_{GT} \quad (2)$$

However, in reality, there is a difference between the impacts of η_{GT} and η_{ST} on η_{CCPP}, because η_{GT} does not depend on η_{ST}, whereas the theoretical maximum of η_{ST} depends on η_{GT}. At a constant gas-turbine inlet temperature, η_{ST} is inversely proportional to η_{GT} because an increase of η_{GT} reduces the output flue-gas temperature from the gas turbine and thus reduces the average temperature of the heat delivered to the steam-turbine cycle. Carefully examining Eq. (1) reveals that the bottom cycle would not have an available heat ratio of $1 - \eta_{GT}$ but would be reduced by the loss of radiation owing to the temperature difference between the outer casing of the gas turbine and the environment, the losses in the gas-turbine electrical generator, and other mechanical losses. Because of their minor impact on η_{GT}, these losses are not considered [21]. Considering them is not necessary for this study, because the amount of heat delivered to the HRSG is represented by the HRSG flue-gas inlet temperature, i.e., only η_{ST} is optimized, which indirectly affects the increase of η_{CCPP}.

The thermodynamic efficiency of the steam-turbine part of the combined cycle is

$$\eta_{ST} = \eta_{SC} \cdot \eta_{HRSG} \quad (3)$$

The thermodynamic efficiency of the steam-turbine cycle is

$$\eta_{SC} = \frac{(P_{ST} - P_{FP})}{\Phi_{HRSG,ex}} \quad (4)$$

The thermodynamic efficiency of the HRSG is

$$\eta_{HRSG} = \frac{\Phi_{HRSG,ex}}{\Phi_{HRSG,in}} \quad (5)$$

η_{SC} depends on the fresh steam temperature and the condensation temperature. To increase η_{SC}, the temperature of the fresh steam should be as high as possible and the condensation temperature should be as low as possible, in accordance with Carnot's theorem. Heat exchangers in HRSGs are arranged in a network. In the direction of the flue gas stream, there is an arbitrary series of heat exchangers. Each of the series represents a different steam-pressure level or steam-reheater level. Because the reheating behaves as a separate steam cycle, each reheating level must provide an additional series of heat exchangers in the heat-exchanger network. Fig. 2 schematically shows the steam turbine plant with three pressure levels (high pressure (HP), intermediate pressure (IP), and low pressure (LP)) and the high-pressure reheater (RH). This setup allows a parallel arrangement of any two or more heat exchangers belonging to different steam-pressure levels or reheating levels.

To ensure the arbitrary positioning of heat exchangers with different pressure levels, a sufficient number of heat exchangers in each series was necessary. This way, any mutual position combination of heat exchangers could be described, in both the serial and parallel directions. An optimization program determined the enthalpy increment in each heat exchanger. The enthalpy increment could be equal to zero, which means that in this position, there was no heat exchanger. Thus, the optimization routine determined the configuration of the HRSG.

Because the thermodynamic efficiency of a steam turbine strongly affects the mechanical energy produced in the turbine, it was necessary to avoid an erroneous calculation of the produced mechanical energy, which occurs if the produced energy is calculated as a result of the multistage expansion in the turbine. For a multistage expansion turbine, the produced mechanical energy is higher than that in the case of a single expansion turbine. If the energy produced for a single expansion turbine is calculated, the erroneous calculation is avoided, as is case in this study. This is why each pressure level has its own turbine. This way, the calculation of the multistage expansion in the turbine is avoided; each pressure level expands from the working pressure to the condensation pressure. The problem with multistage/single expansion in turbines is well-known in turbomachinery theory [22]. To simplify the calculation, in this study, the thermodynamic efficiency of the turbine is set to be constant and equal to 90%, which is a typical approach [23].

The water and flue-gas pressure reductions are ignored because they depend on the geometrical characteristics of the steam generator and are somewhat independent of the heat-exchanger arrangement. The flue-gas pressure reduction can be reduced by decreasing the flue-gas speed and increasing the cross sectional

Please cite this article in press as: Čehil M et al. Novel method for determining optimal heat-exchanger layout for heat recovery steam generators. Energy Convers Manage (2017), http://dx.doi.org/10.1016/j.enconman.2017.03.033

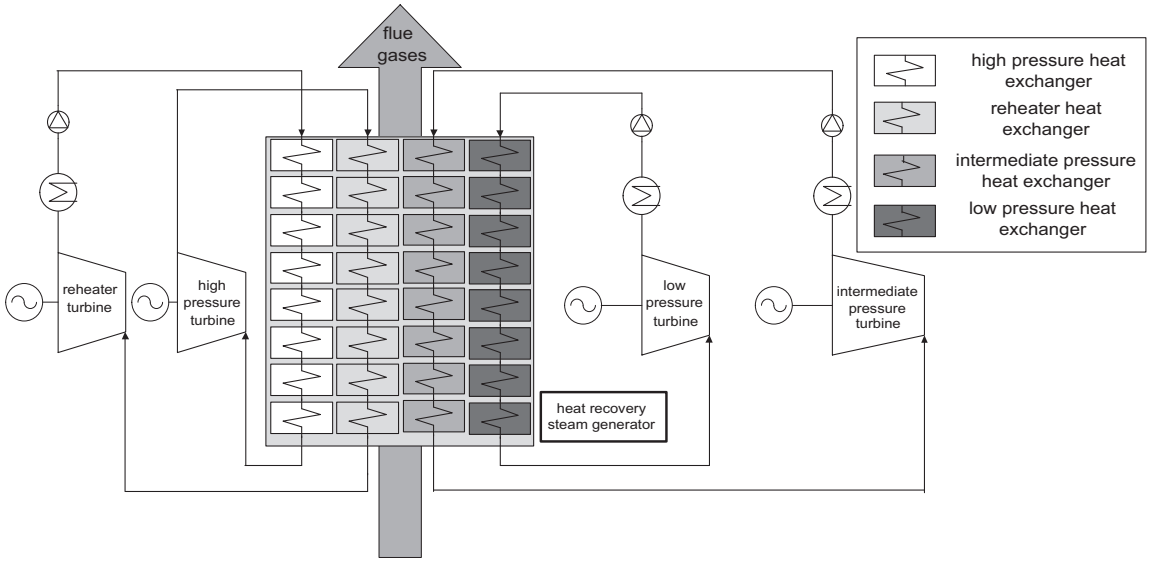

Fig. 2. Schematic of the steam-turbine power plant.

area of the steam generator. The water-pressure reduction can be decreased by increasing the number of parallel lines in each heat exchanger. Such calculations are in a lower hierarchical order of optimization [24] and are therefore not covered in this paper. Because of the large number of objective-function calculations required, which reaches several hundred thousand for just one optimization, the mathematical model must be simplified as much as possible in order to perform the optimization in real time and obtain physically feasible solutions. The mathematical model was written in MATLAB, and the optimization was performed using the MATLAB genetic algorithm optimization toolbox. Xsteam tables were used for the water/steam physical properties. A simplified schematic of the calculation algorithm is shown in Fig. 3.

The basic algorithm equations are given as follows:

(a) for the i^{th} working-fluid pressure level (from the HRSG outlet towards the HRSG inlet):

$$h_{wf,i}(j+1) = h_{wf,i}(j) + \Delta h_i \tag{6}$$

$$T_{wf,i}(j+1) = f(h_{wf,i}(j+1), p_{wf,i}) \tag{7}$$

$$\Phi_{wf,i}(j+1) = \Phi_{wf,i}(j) + \Delta h_i \cdot q_{m_i}, \tag{8}$$

where

$$q_{m_{(i+1)}} = x_i \cdot q_{m_1} \tag{9}$$

(b) for the j^{th} element of flue gas (from the HRSG inlet towards the HRSG outlet):

$$h_{fg}(j+1) = h_{fg}(j) + \sum_{k=1}^{n} \frac{q_{m_1} \cdot \Delta h_k}{1 - g_{rad}} \tag{10}$$

$$T_{fg}(j+1) = f(h_{fg}(j+1)) \tag{11}$$

$$\Phi_{fg}(j+1) = \Phi_{fg}(j) + \sum_{k=1}^{n} \frac{\Delta h_k \cdot q_{m_k}}{1 - g_{rad}} \tag{12}$$

(c) for calculating the pinch point:

$$\Delta T_{pp,i}(j) = T_{fg,i}(j) - T_{wf,i}(j) \tag{13}$$

The constraint is

$$\min(\Delta T_{pp,i}) = 0 \tag{14}$$

Special attention was paid to finding the pinch point. The pinch point mostly occurs at the water entrance to the evaporator, but at higher pressures, the pinch point moves towards the economizer. Because the water/steam and flue-gas conditions are known only at the ends of the heat exchangers, if the pinch point is set at the beginning of the evaporator, a physically impossible solution is obtained and the calculation yields incorrect results because the calculated rates of the mass flow through the steam generator are higher than what is physically possible. Therefore, determining a real pinch point is very important for an accurate mathematical model. Each heat exchanger prior to the evaporator for each pressure level was divided into 50 parts; thus, a more accurate temperature profile of water was obtained. For each calculated mass flow rate of the first pressure level, the enthalpy and temperature profile of steam and flue gas were determined. The mass flow rates of the other pressure levels were already determined by their proportion in the mass flow of the first pressure level and represented additional independent variables. Then, the temperature differences between the flue gas and water/steam at the end of the heat exchangers were calculated. The minimum of these differences was the pinch point. When the pinch point decreases to zero, the greatest possible mass flow rate is established. Each pressure level has its own steam turbine, in which steam can expand to the condenser pressure. If the dryness fraction at the steam-turbine outlet is less than 80%, the steam expands to a higher pressure, at which the dryness fraction is exactly 80%. The dryness fraction [27] is a boundary condition imposed in the mathematical model. Such a penalty has proven to be very effective for obtaining optimal solutions because it avoids further constraints. The fuel used in the calculation was natural gas, and its content is shown in Table 1. The input data are shown in Table 2.

3. Results

In this chapter, the optimization results for different HRSG configurations (single pressure (SP), SP with reheater (SP + RH), double pressure (DP), DP with reheater (DP + RH), TP, and TP with reheater (TP + RH)) are presented.

3.1. SP HRSG configuration

Fig. 4 shows a T–Φ diagram of the thermodynamically optimized steam turbine plant. In the simplest case, there is no

Please cite this article in press as: Čehil M et al. Novel method for determining optimal heat-exchanger layout for heat recovery steam generators. Energy Convers Manage (2017), http://dx.doi.org/10.1016/j.enconman.2017.03.033

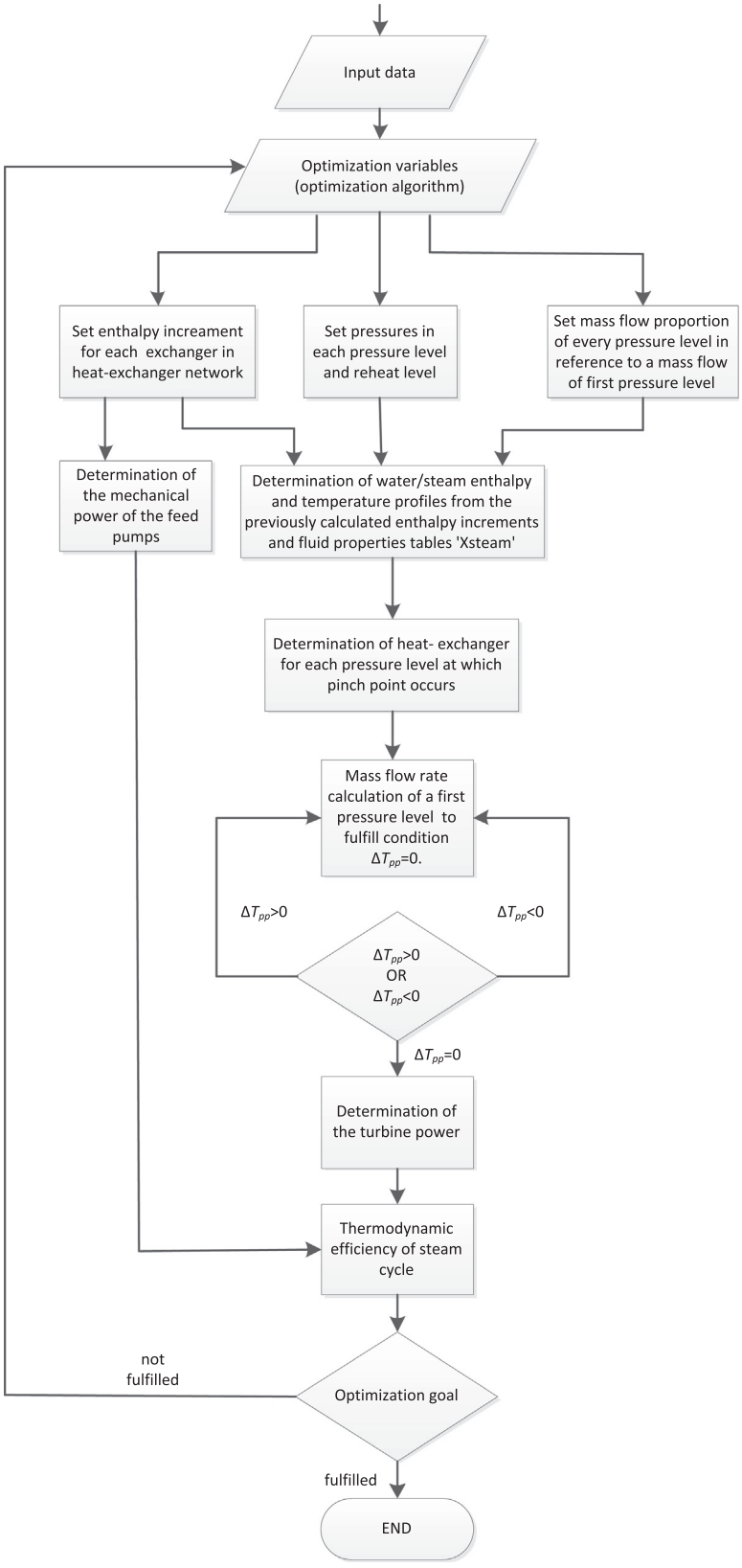

Fig. 3. Simplified calculation algorithm flow chart.

possibility of a parallel arrangement of heat exchangers. Thus, the optimization is easy—only the vapor pressure must be specified in order to determine the minimum allowed dryness fraction at the turbine outlet at the maximum fresh steam temperature of 565 °C. Fig. 4 also shows that the pinch point is not at the point of the saturated liquid but is located within the economizer. In the case of an SP configuration and zero pinch point, it is impossible to cool the flue gases below 128 °C. The detailed results for each

Please cite this article in press as: Čehil M et al. Novel method for determining optimal heat-exchanger layout for heat recovery steam generators. Energy Convers Manage (2017), http://dx.doi.org/10.1016/j.enconman.2017.03.033

Table 1
Fuel content.

Component	Vol. %
Methane (CH_4)	85.0
Ethane (C_2H_6)	5.0
Propane (C_3H_8)	3.0
Carbon dioxide (CO_2)	3.5
Nitrogen (N_2)	3.5
Hydrogen sulfide (H_2S)	0.0

Table 2
Input data.

	Value
Maximum steam temperature [24]	565 °C
Maximum pressure water/steam	1000 bar
Inlet flue-gas temperature [25]	600 °C
Mass flow of flue gas	1 kg/s
Steam condensation temperature	25 °C
Feed-pump efficiency [26]	84%
Steam-turbine efficiency	90%
HRSG heat losses to the environment [6]	0.5%
Mechanical and electrical losses [26]	2%

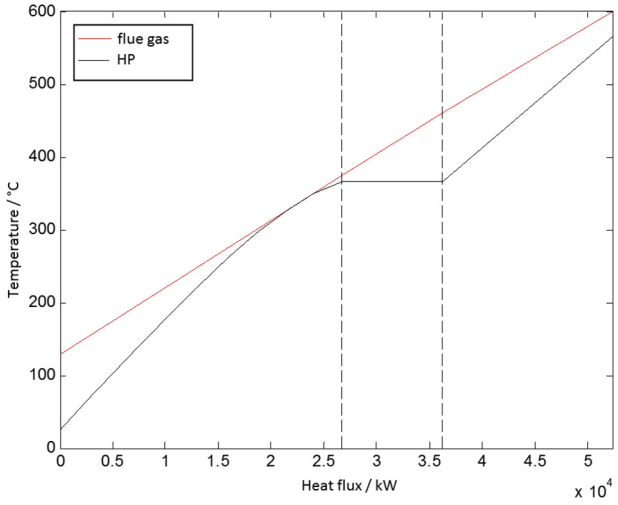

Fig. 4. T–Φ diagram for the thermodynamically optimized SP HRSG configuration.

calculated HRSG configuration presented in this paper are shown in Table 3.

3.2. SP+RH HRSG configuration

The optimization results for the SP + RH HRSG configuration are identical to those for the SP configuration. Because of the small temperature difference between the flue gas entering the HRSG and the maximum steam temperature at the HRSG outlet (35 °C), there is not enough available heat flow to be used for reheating. The model shows that the introduction of the reheater to the HRSG with one pressure level is thermodynamically justified only with an increased inlet temperature of the flue gas entering the HRSG.

3.3. DP HRSG configuration

Fig. 5 shows a *T–Φ* diagram of the thermodynamically optimized DP HRSG configuration. The HP level is identical to that for an SP configuration without a reheater, whereas the LP level has a higher dryness fraction at the steam-turbine outlet. In Fig. 4, which shows the *T–Φ* diagram for the SP configuration, the pinch point is at a temperature slightly above 300 °C. Below this temperature, the water curve separates from the flue gas curve, which means that at temperatures below approximately 310 °C, there is available thermal flow that cannot be used in the SP configuration. This thermal flow is used by the second pressure level. For this reason, the flue gas is cooled to 55.2 °C.

3.4. DP+RH HRSG configuration

Fig. 6 shows a *T–Φ* diagram of the thermodynamically optimized DP + RH configuration. The parallel arrangement of heat exchangers is almost always used. The introduction of the reheater to a DP HRSG causes a drastic pressure increase in the HP level. To achieve better results, calculations with different initial conditions were performed. The results exhibited relatively small deviations of η_{ST}, although the HRSG configurations and operating parameters differed. According to these calculations, there are many solutions with similar η_{ST} values. The LP level varies from 2 to 10 bar, and the HP steam pressure is approximately 430 bar.

3.5. TP HRSG configuration

Fig. 7 shows a *T–Φ* diagram for a thermodynamically optimized steam turbine plant with three pressure levels (TP) without a reheater. In this case, as well as for the TP HRSG configuration, genetic algorithms rarely change the initial pressures of the lower pressure levels. The IP and LP levels, because of the reduced flow rate of water/steam compared with the water/steam mass flow rate of the HP pressure level and their lower η_{SC}, have a smaller impact then the HP level on η_{ST}. To obtain the best possible solution, several calculations were performed with different IPs and LPs as the initial conditions. The optimal pressures reported by other authors were also considered. Bassily [26] states that the optimal pressures of the IP and LP levels were fairly constant and, for the thermodynamically optimized (TP + RH) HRSG configuration, their values were 4.5 and 1.2 bar, respectively. For the TP HRSG configuration with and without a reheater, this combination of pressures yielded the best solution among several different combinations. The differences in the thermodynamic efficiency varied by no more than 0.2% in absolute value, confirming previously stated assumptions that there are numerous pressure combinations of lower pressure levels that yield very similar solutions.

3.6. TP+RH HRSG configuration

Fig. 8 shows a *T–Φ* diagram for the thermodynamically optimized TP + RH HRSG configuration.

The thermodynamic efficiency of this plant is the highest among all the plants considered thus far. The *T–Φ* diagram shows that all the temperature curves at the pinch points adhere to the flue-gas temperature curve, which indicates good utilization of the waste heat in the HRSG. Additionally, there is a maximum possible matching of the reheater temperature curve with the temperature curves of the HP economizer and superheater, which suggests that this is a thermodynamically well-optimized configuration.

In this case, η_{ST} is larger than that in the TP configuration, despite the fact that flue-gas outlet temperature is higher than that in the TP case. As previously stated, η_{ST} is the product of η_{HRSG} and η_{SC} (Eq. (3)). A large η_{HRSG} is insufficient to achieve a large η_{ST}. For example, the steam generator can have a very high value of the working-fluid flow. The flue gas is cooled to a temperature that is almost equal to the temperature of the working fluid at the entrance to the HRSG, and the working-fluid temperature at the HRSG outlet is slightly higher than that at the HRSG entrance

Table 3
Results for single, double, and triple-steam pressure level HRSGs with and without reheating.

		Unit	SP	SP + RH	DP	DP + RH	TP	TP + RH
	No. of variables		5	10	17	25	32	42
	No. of serial heat exchangers		3	3	6	6	8	8
	No. of parallel heat exchangers		1	2	2	3	3	4
	Exchanged heat flux	kW/kg_{FG}	522.81	522.81	599.50	584.04	608.68	602.84
	Flue gas enthalpy (outlet)		134.19	134.19	57.50	72.96	48.32	54.16
	η_{SC}	%	39.99	39.99	37.81	39.57	37.64	38.71
	η_{HRSG}	%	79.58	79.58	91.25	88.89	92.65	91.76
	η_{ST}	%	31.82	31.82	34.50	35.18	34.87	35.52
	$\eta_{exergy,total}$	%	71.8	71.8	77.8	79.4	78.6	80.1
	Flue gas outlet temp.	°C	128.25	128.25	55.17	70.06	46.44	51.95
	Net electrical power	kW/kg_{FG}	210.12	210.12	226.64	231.24	229.06	233.46
HP	Pressure	bar	198.4	198.4	198.0	427.4	198.0	413.8
	Feed water temperature	°C	26.3	26.3	26.3	27.8	26.3	27.7
	Evaporation temperature	°C	365.1	365.1	364.9	425.7	364.9	423.2
	Live steam temperature	°C	565.0	565.0	565.0	565.0	565.0	565.0
	Steam mass flow	$(kg/s)/kg_{FG}$	0.157	0.157	0.157	0.128	0.157	0.127
	Electrical power	kW/kg_{FG}	212.82	212.82	212.43	45.29	212.34	41.77
	Feed-pump power	kW/kg_{FG}	2.70	2.70	3.69	6.45	3.69	6.2
	Wet-steam ratio (turb. outlet)	%	20.0	20.0	20.0		20.0	
RH	Reheating pressure	bar				76.9		88.3
	Reheating temperature	°C				565.0		565.0
	Pinch point	°C				2.4		1.0
	Steam mass flow	$(kg/s)/kg_{FG}$				0.128		0.127
	Electrical power	kW/kg_{FG}				168.2		168.4
	Wet-steam ratio (turb. outlet)	%				13.6		14.4
IP	Pressure	bar					4.5	4.0
	Feed water temperature	°C					25.1	25.1
	Evaporation temperature	°C					147.9	147.9
	Live steam temperature	°C					318.2	240.3
	Steam mass flow	$(kg/s)/kg_{FG}$					0.022	0.038
	Electrical power	kW/kg_{FG}					16.52	26.31
	Feed-pump power	kW/kg_{FG}					0.01	0.02
	Wet-steam ratio (turb. outlet)	%					8.5	12.4
LP	Pressure	bar			3.0	5.0	1.2	1.2
	Feed water temperature	°C			25.0	25.0	25.0	25.0
	Evaporation temperature	°C			133.5	152.1	104.8	104.8
	Live steam temperature	°C			306.9	152.7	276.9	144.7
	Electrical power	kW/kg_{FG}			17.9	24.2	3.9	3.2
	Feed-pump power	kW/kg_{FG}			0.0	0.0	0.0	0.0
	Wet-steam ratio (turb. outlet)	%			7.0	18.3	3.6	10.7

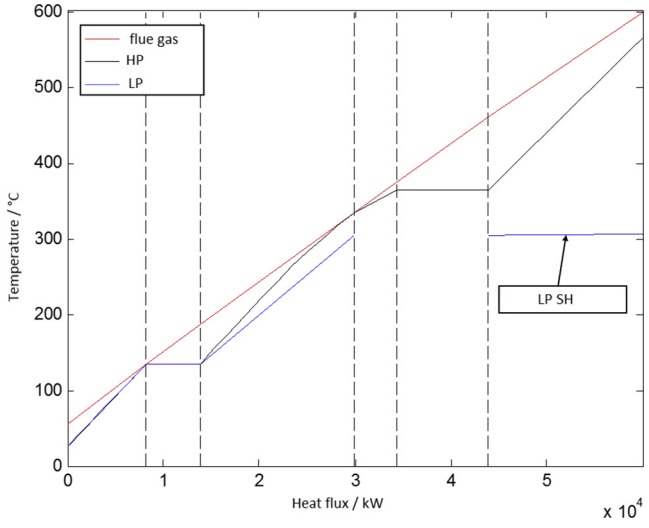

Fig. 5. T–Φ diagram for the thermodynamically optimized TP HRSG configuration.

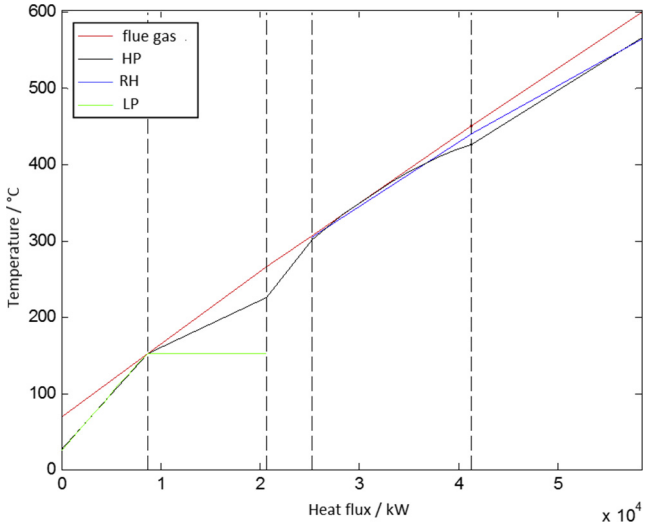

Fig. 6. *T–Φ* diagram for the thermodynamically optimized TP + RH HRSG configuration.

(Fig. 9). In this case, η_{HRSG} is as high as possible, but η_{SC} is zero because the working fluid does not achieve evaporation and thus electricity is not produced in the steam turbine.

The introduction of a reheater requires heat exchange at higher temperatures, which necessitates the reduction of the working-fluid flow of a higher pressure level compared with an HRSG without a reheater. The low pressure level in both cases (TP + RH and TP) is the same (same pressure), as is the temperature at which the pinch point occurs. The total working-fluid flow (all three

Please cite this article in press as: Čehil M et al. Novel method for determining optimal heat-exchanger layout for heat recovery steam generators. Energy Convers Manage (2017), http://dx.doi.org/10.1016/j.enconman.2017.03.033

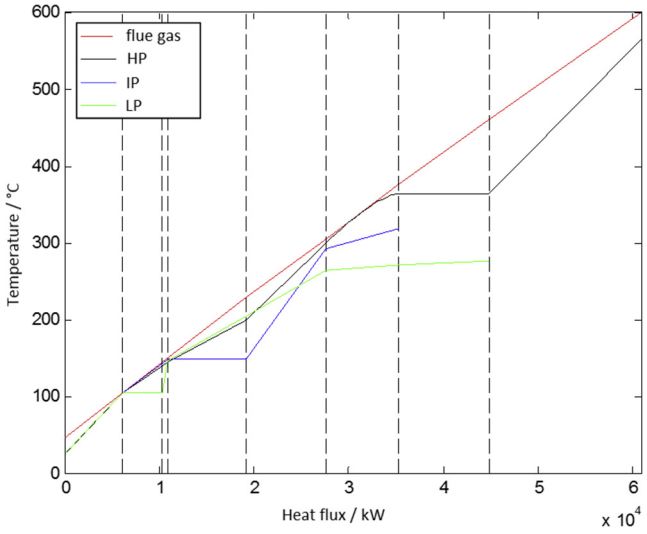

Fig. 7. T–Φ diagram for a thermodynamically optimized plant with the TP HRSG configuration.

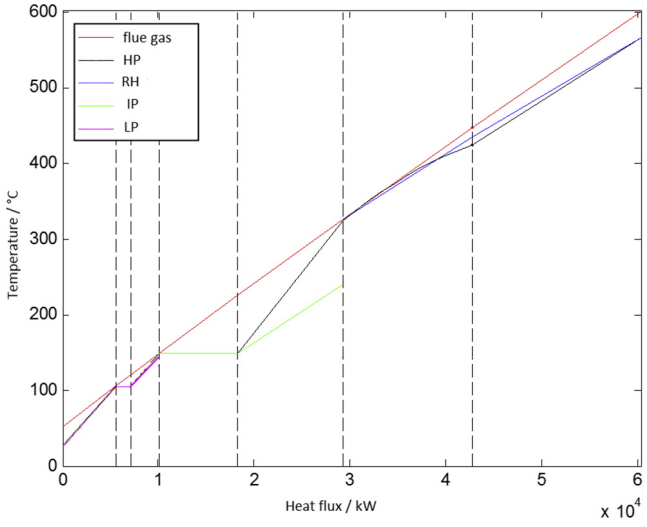

Fig. 8. T–Φ diagram for a thermodynamically optimized plant with the TP + RH HRSG configuration.

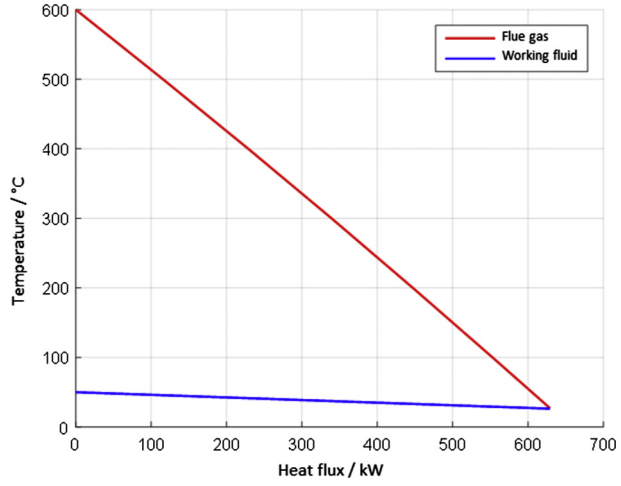

Fig. 9. T–Φ diagram for an HRSG with a very high working-fluid flow at the first pressure level.

pressure levels) is lower for TP + RH than for TP, and this is why the flue gas cannot be cooled to the temperature for the TP case. Despite this phenomenon, by the introduction of a reheater, the average η_{ST} of a power plant increases (the mean effective temperature of the heat increases). The conclusion is that the introduction of a reheater has a greater overall impact (positive: η_{ST} increases) on η_{ST} than η_{HRSG} has (negative: η_{ST} decreases).

4. Conclusion

The newly developed mathematical model allows the simultaneous determination of the optimal heat-exchanger layout and the optimal operating parameters of the steam-turbine part of a combined power plant for any flue-gas temperature at the gas turbine outlet. In contrast, in previous studies by other researchers, the heat-exchanger layout was determined in advance according to previous experience, and only the operational parameters were optimized. The mathematical model presented in this paper allows for the parallel arrangement of any two or more heat exchangers belonging to different steam pressure levels or reheating levels. The analysis was performed for a flue-gas temperature of 600 °C, which is the approximate temperature currently practically used at the gas turbine outlet. With regard to the maximum temperatures, such a plant is currently feasible, but the high thermodynamically optimal pressure of fresh steam, which is greater than 400 bar if the plant has reheating, is problematic. According to Eq. (1), to increase the thermodynamic efficiency of a combined power plant with three pressure levels and a reheater (approximately 60%), η_{GT} should be greater than 38%, but because the η_{ST} of a thermoeconomic optimal plant is lower than 35.52%, which is the thermodynamic maximum, η_{GT} should be increased. As shown in Table 3, the introduction of additional pressure levels reduces the average η_{ST} of a cycle but allows the significant increase of η_{HRSG}, which results in an increase of η_{ST}. By using the proposed optimization method, a large η_{HRSG} with the maximum possible average η_{ST} can be determined. η_{ST} depends strongly on the properties of the working fluid, and because η_{HRSG} almost reaches its maximum, the emphasis for the increase of η_{ST} should be placed on the increase of the average η_{ST}, which—along with the temperature increase at the gas turbine inlet—is the only factor that can increase η_{CCPP}. It has been shown that for a flue-gas temperature of 600 °C, the supercritical pressures are thermodynamically optimal only in plants with reheating, whereas in plants without reheating, thermodynamically optimal pressures are subcritical. This is because of the properties of water as a working fluid and the fact that to achieve the maximum η_{ST}, it is necessary to achieve the maximum allowable moisture content at the steam-turbine outlet. In this study, the maximum allowable moisture content was considered to be 20%, which is similar to the value used by other researchers. A reduction of the maximum allowable moisture content would result in a lower thermodynamically optimum pressure of the HP steam, which is closer to the design solutions. The introduction of a reheater to cycles with two or three pressure levels increases η_{ST}, whereas the introduction of a reheater to cycles with a single pressure level reduces η_{ST} because the temperature difference between the flue-gas inlet temperature and the temperature of the pinch point is small, which indicates insufficient heat flux for the simultaneous superheating and reheating of steam. In this case, the impact of the η_{HRSG} reduction is more significant than the impact of the η_{ST} increase. The same occurs in cycles with two or three pressure levels, but here, the second and third pressure levels increase η_{HRSG} along with the higher average η_{ST} of all the pressure levels. The optimal solutions for the heat-exchanger position often involve a parallel arrangement of heat exchangers within the HRSG. The obtained results are not

the outcome of assumptions but rather a direct result of the optimization process. Some researchers have used parallel arrangements of heat exchangers, but most researchers do not realize the thermodynamic benefits of this approach and exclusively use serial heat-exchanging surfaces.

References

[1] <https://ec.europa.eu/clima/policies/strategies/2020_en>.
[2] <http://www.siemens.com/press/en/feature/2011/energy/2011-09-irsching4.php>.
[3] <https://powergen.gepower.com/about/insights/power-plant-efficiency-record.html>.
[4] Kehlhofer R. Combined-cycle gas and steam power plants. Tulsa, USA: PennWell Corporation; 2009.
[5] Nadir M, Ghenaiet A. Thermodynamic optimization of several (heat recovery steam generator) HRSG configurations for a range of exhaust gas temperatures. Energy 2015;86:685–95.
[6] Ganapathy V. Industrial boilers and heat recovery steam generators design, applications and calculations. New York: Marcel Dekker Inc; 2002.
[7] Valdes M, Duran D, Rovira A. Thermoeconomic optimization of combined cycle gas turbine power plants using genetic algorithms. Appl Therm Eng 2003;23:2169–82.
[8] Kotowicz J, Bartela L. The influence of economic parameters on the optimal values of the design variables of a combined cycle plant. Energy 2010;35:911–9.
[9] Rahim M. Thermodynamic evaluation and parametric study of a combined cycle power plant: application for Ankara city. J. Energy Eng. 2013. http://dx.doi.org/10.1061/(ASCE)EY.1943-7897.0000127.
[10] Feng H, Zhong W, Wu Y, Tong S. Thermodynamic performance analysis and algorithm model of multi-pressure heat recovery steam generators (HRSG) based on heat exchangers layout. Energy Convers Manage 2014;81:282–9.
[11] Naemi S, Saffar-Avval M, Kalhori SB, Mansoori Z. Optimum design of dual pressure heat recovery steam generator using non-dimensional parameters based on thermodynamic and thermoeconomic approaches. Appl Therm Eng 2013;52:371–84.
[12] Mansouri TM, Ahmadi P, Kaviri AG, Jaafar MNM. Exergetic and economic evaluation of the effect of HRSG configurations on the performance of combined cycle power plants. Energy Convers Manage 2012;58:47–58.
[13] Rovira A, Sanchez C, Munoz M, Valdes M, Duran MD. Thermoeconomic optimization of heat recovery steam generators of combined cycle gas turbine power plants considering off-design operation. Energy Convers Manage 2011;52:1840–9.
[14] Verkhivker G, Kosoy B. On the exergy analysis of power plants. Energy Convers Manage 2001;42:2053–9.
[15] Bejan A, Tsatsaronis G, Moran M. Thermal design and optimization. New York: John Wiley & Sons Inc; 1996.
[16] Mert MS, Dilmac OF, Ozkan S, Karaca F, Bolat E. Exergoeconomic analysis of a cogeneration plant in an iron and steel factory. Energy 2012;46:78–84.
[17] Baghernejad A, Yaghoubi M. Exergoeconomic analysis and optimization of an Integrated Solar Combined Cycle System (ISCCS) using genetic algorithm. Energy Convers Manage 2011;52:2193–203.
[18] Ahmadi P, Dincer I. Thermodynamic analysis and thermoeconomic optimization of a dual pressure combined cycle power plant with a supplementary firing unit. Energy Convers Manage 2011;52:2296–308.
[19] Petrakopoulou F, Tsatsaronis G, Morosuk T, Carassai A. Conventional and advanced exergetic analyses applied to a combined cycle power plant. Energy 2012;41:146–52.
[20] Carapelluci R, Giordano L. A comparison between exergetic and economic criteria for optimizing the heat recovery steamgenerators of gas-steam power plants. Energy 2013;58:458–72.
[21] Kehlhofer R. Combined-cycle gas steam turbine power plants. 3rd ed. Tulsa: PennWell Corp., USA; 2009.
[22] Dixon SL. Fluid mechanics, thermodynamics of turbomachinery. Oxford: Butterworth-Heinemann; 1998.
[23] Franco A. Casarosa Cthermoeconomic evaluation of the feasibility of highly efficient combined cycle power plants. Energy 2004;29:1963–82.
[24] Franco A, Russo A. Combined cycle plant efficiency increase based on the optimization of the heat recovery steam generator operating parameters. Int J Therm Sci 2002;41:843–59.
[25] Franco A, Casarosa C. On some perspectives for increasing the efficiency of combined cycle power plants. Appl Therm Eng 2002;22:1501–18.
[26] Bassily AM. Modeling, numerical optimization and irreversibility reduction of a triple-pressure reheat combined cycle. Energy 2007;32:778–94.
[27] Casarosa C, Donatini F, Franco A. Thermoeconomic optimization of heat recovery steam generators operating parameters for combined plants. Energy 2004;29:389–414.

Please cite this article in press as: Čehil M et al. Novel method for determining optimal heat-exchanger layout for heat recovery steam generators. Energy Convers Manage (2017), http://dx.doi.org/10.1016/j.enconman.2017.03.033